# Fermi National Accelerator Laboratory

FERMILAB-FN-657

# Electron Cooling in High Energy Colliders

S.Y. Lee, P. Colestock and K.Y. Ng

*Fermi National Accelerator Laboratory*
*P.O. Box 500, Batavia, Illinois 60510*





June 1997

Operated by Universities Research Association Inc. under Contract No. DE-AC02-76CH03000 with the United States Department of Energy

## Disclaimer



## Distribution

FN-657

# Electron Cooling in High Energy Colliders

S.Y. Lee,* P. Colestock, and K.Y. Ng

*Fermi National Accelerator Laboratory,† P.O. Box 500, Batavia, IL 60510*

(June, 1997)

## Abstract

The feasibility of employing electron storage rings to cool ions in storage rings and colliders is presented. Cooling rates are estimated. The dynamical cooling equations are studied with radiation damping and intrabeam scattering taken into account. We find that the electron-storage-ring concept can be used to cool protons (antiprotons) in the Tevatron, and ions in RHIC efficiently and economically.

*On leave from the Department of Physics, Indiana University at Bloomington, IN 47405.

†Operated by the Universities Research Association, Inc., under contract with the U.S. Department of Energy.

# I. INTRODUCTION

Since its invention by G.I. Budker in 1966, electron cooling [1] has been widely applied to many low-energy storage rings for atomic, nuclear, particle [2], and accelerator physics research [3, 4, 5, 6, 7, 8]. Heuristically, the electron-cooling force can be viewed as a frictional force resulting from the heat exchange between the hot ions and cold electrons. In the rest frame of the electrons, ions with higher or lower velocities than those of the nearly equal-speed electrons have to travel forward or backward through the cold electron cloud in the electron-cooling section. Since the charged ions lose energy in passing through the electron cloud, the ions will be slowed down relative to the rest frame of the electron beam. The frictional force is particularly effective if the velocity difference between ions and cooling electrons is small. Since the velocities of the electrons and ions are nearly equal, a very thin target of cooling electrons, of the order of $10^{10}$ e/cm$^2$, can efficiently damp the ion-beam oscillations and sustain the diffusion process equivalent to a fixed internal target having a thickness of about $10^{16}$ charges/cm$^2$ [2].

In storage rings and high-energy colliders, the demand of higher beam brightness requires intricate beam manipulations. In particular, the employment of beam cooling to compensate for the heating processes such as intrabeam scattering, beam-beam interaction, beam gas scattering etc., can enhance beam lifetime and luminosity.

For example, in order to achieve high luminosity at the Fermilab TeV collider—the Tevatron, the Recycler has been proposed to recycle unused antiprotons from the Tevatron [9]. The recycled antiprotons can be cooled by stochastic cooling or electron cooling to attain a high phase-space density in the Recycler. At the same time, the Recycler accumulates newly produced, pre-cooled antiprotons from the antiproton Accumulator.

When the Main Injector and the Recycler are put into service, the intensity of antiprotons can be significantly increased. With the addition of the beam cooling, beam brightness can be enhanced to attain higher initial luminosity in the Tevatron. However, the intense beam bunches in Tevatron still suffer emittance growth in both the longitudinal and transverse directions due to intrabeam scattering, and other beam-diffusion processes.

Similarly, the effect of intrabeam scattering is particularly severe at the relativistic heavy ion collider (RHIC) presently under construction at the Brookhaven National Laboratory. To maintain beam stability, a high-voltage rf system has to be employed in order to confine beam particles inside the stable region.

One would ask the question: can the beams in colliders be cooled to preserve their brightness? There have been attempts to cool (anti)proton bunches at the Tevatron by stochastic cooling methods [10]. However, in order for stochastic cooling to proceed, one requires a beam detection system that can provide Schottky signal without the contamination of any coherent beam signals. Unfortunately, the observed Schottky signal at the Tevatron was dominated by coherent bunched beam signals.

Alternately, electron cooling of high-energy hadron beams has also been investigated [11]. Rubbia [12] and Ruggiero [13] proposed electron cooling for antiproton collection, and Ellison [14] proposed electron cooling for colliders. Rubbia outlined the electron cooling of the CERN SPS at about 300 GeV using an electron storage ring, while Ruggiero applied Rubbia's idea to the Fermilab Main Ring operating at 200 GeV. They put emphasis on cooling in the transverse directions, which was hard to accomplish. Ellison's proposal was to use the electron source from a pelletron or similar dc devices. Unfortunately, a dc electron source with sufficient high current and energy for the cooling process is not currently available. The key question is, do we need a dc electron source for beam cooling? Can we employ the known technology of electron storage rings for high-energy ion beam cooling?

For low-energy beams operated below the transition energy, the diffusion rate of multiple Coulomb scattering is high [15]. One needs a very strong cooling force to maintain beam stability. For high-energy storage rings or colliders operated above the transition energy, the diffusion rate of multiple Coulomb scattering is considerably smaller and is almost energy independent. In addition, the size of a high-energy beam is small. We therefore hope that an electron beam of relatively low current would be adequate to achieve a high electron density to compensate for the diffusion processes and maintain the beam brightness of the storage ring or the luminosity of the collider.

This paper studies the feasibility of using electron storage rings for beam cooling in hadron storage rings and colliders. Most storage rings and colliders have been designed so that the intensity of the beams is not much below the collective instability

limits and the beam-beam tune shift limits. Therefore, it is not our intention to cool the beams to much lower emittances; what we want is to preserve them instead. We also notice that the longitudinal emittance of a storage ring or collider grows much faster than the transverse emittances. Taking the Tevatron as an example, the e-folding growth time of the longitudinal emittance is of the order of one hour, while the growth time of the transverse emittance is of the order of 8 to 9 hrs, which is the length of a typical store [16]. This is because, first, the longitudinal beam temperature is very much lower than the transverse temperatures as a result of energy ramping, and second, the heat in the transverse coordinates is being continually transferred to the longitudinal coordinate, although possibly at a low rate, through processes like intrabeam scattering [15] and Touschek scattering [17]. Therefore, it is the longitudinal emittance that we need to cool. We suggest using an electron ring having the same rf frequency as the storage ring or collider, and sharing a common straight section where the cooling takes place. The bucket spacing of the electron ring should be an integral multiple of the bucket spacing of the ion storage ring. In other words, we must have

$$\frac{C_e}{h_e} = n\frac{C_i}{h_i} \qquad n \text{ an integer} , \tag{1.1}$$

where $C_e$ and $C_i$ are, respectively, the circumferences of the electron and ion rings, and $h_e$ and $h_i$ their respective rf harmonics. A schematic drawing of the cooling system is shown in Fig. 1.

The lattice of the electron ring has to be specially designed to have a short radiation damping time so that the cool temperatures of the electrons can be replenished reasonably fast. To be effective in cooling, we also require that the natural transverse beam sizes match those of the ion bunches to be cooled. At the same time, the rf in the electron ring must provide a bunch length to match those of the ion bunches.

Section II reviews briefly the basic properties of an electron beam in a storage ring and discusses the temperatures and resulting cooling force. Section III examines the possible cooling scenarios in the Tevatron, the Recycler, and RHIC. Because of the high charge of the ions in RHIC, the transverse emittance of the ion beam grows rather rapidly as a result of intrabeam scattering. However, these ion bunches are stored at only 100 GeV per nucleon. At such low gamma $\gamma$, the total energy divided by the rest mass, the cooling electrons will have a much lower transverse temperature

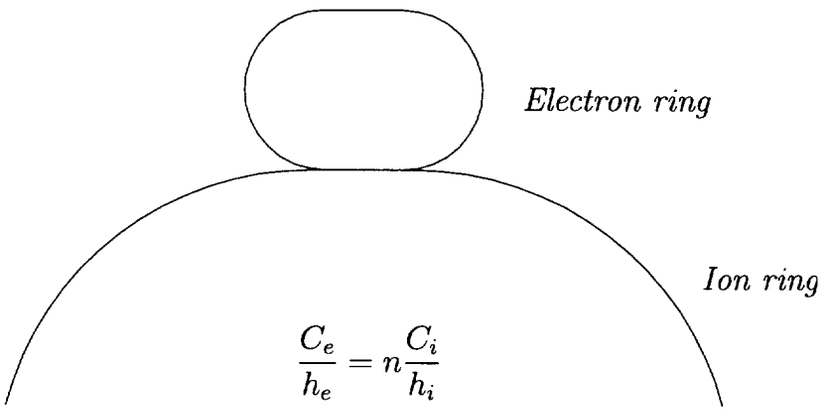


Figure 1. A schematic drawing of the ion storage ring and its corresponding cooling electron storage ring. The bucket spacing of the electron ring should be an integral multiple of the bucket spacing of the ion storage ring. Therefore, we must have $nh_eC_i = h_iC_e$, where $n$ is an integer, $C_e$ and $C_i$ are, respectively, the circumferences of the electron and ion rings, and $h_e$ and $h_i$, their respective rf harmonics.

making transverse cooling of the ion bunches also possible. Section IV addresses the dynamics of electron cooling taking into account radiation damping and intrabeam scattering. The conclusion is given in Sec. V.

# II. ELECTRON COOLING DRAG FORCE

In this section, we review some basic properties of an electron beam in a storage ring and estimate the cooling force given to the ions.

## A. PROPERTIES OF ELECTRONS IN STORAGE RINGS

The power radiated by a relativistic electron at energy $E$ is given by

$$P_\gamma = C_\gamma \frac{cE^4}{2\pi\rho^2} = \frac{e^2c^3}{2\pi} C_\gamma E^2 B^2, \tag{2.1}$$

where $B$ is the magnetic flux intensity, $\rho$ is the local radius of curvature, $R$ is the average radius of the electron storage ring, and

$$C_\gamma = \frac{4\pi}{3}\frac{r_e}{(m_ec^2)^3} = 8.85 \times 10^{-5} \left[\frac{\mathrm{m}}{(\mathrm{GeV})^3}\right], \tag{2.2}$$

with $r_e$ being the classical electron radius, $m_e$ the electron mass, and $c$ the velocity of light. For an electron at the synchronous energy $E_0$, the total energy radiated in one revolution is given by

$$U_0 = \frac{C_\gamma E_0^4}{2\pi} \oint \frac{ds}{\rho^2} = C_\gamma \frac{E_0^4}{\rho} \quad \text{(isomagnetic ring)} \ . \tag{2.3}$$

Therefore the average power is given by

$$\langle P_\gamma \rangle = \frac{U_0}{T_0} = C_\gamma \frac{cE_0^4}{2\pi R\rho} \ , \tag{2.4}$$

where $T_0 = c/(2\pi R)$ is the revolution period. The energy loss of the circulating electron beam is compensated by the *longitudinal* electric field supplied by the rf cavities.

Since the higher-energy electrons in a bunch lose more energy than the lower-energy electrons [see Eq. (2.1)], the longitudinal phase space will be damped. Similarly, since the radiation from an electron comes out in a cone with an open angle about $\gamma^{-1}$ around its trajectory, and the energy loss is replenished through the rf cavities in the longitudinal direction, the transverse phase spaces will also be damped.

The resulting radiation damping rates for all the three degrees of freedom are

$$\alpha_x = J_x \frac{\langle P_\gamma \rangle}{2E_0} \ , \quad \alpha_z = J_z \frac{\langle P_\gamma \rangle}{2E_0} \ , \quad \alpha_s = J_s \frac{\langle P_\gamma \rangle}{2E_0} \ , \tag{2.5}$$

where damping partition numbers are

$$J_x = 1 - \mathcal{D} \ , \quad J_z = 1 \ , \quad J_s = 2 + \mathcal{D} \ , \tag{2.6}$$

with

$$\mathcal{D} = \frac{1}{2\pi} \oint D(s) \left[ \frac{1}{\rho^2} + 2K(s) \right]_{\text{dipole}} ds \ , \tag{2.7}$$

$D(s)$ the dispersion function, and $K(s)$ the field gradient in the dipole.

Since the emission of photons is discrete and random, the quantum process causes also diffusion and excitation. The balance between the damping and excitation provides a natural emittance or beam size for the electron beam bunch in the storage ring. The amplitudes of the betatron and synchrotron oscillations are determined by the equilibrium of the quantum excitation arising from the emission of photons

and the rf acceleration fields used in compensating the energy loss of the synchrotron radiation. The normalized natural rms horizontal emittance is given by

$$\epsilon_{\rm nat} = C_q \gamma^2 \frac{\langle \mathcal{H}/|\rho|^3 \rangle}{J_x \langle 1/\rho^2 \rangle} \ , \tag{2.8}$$

where

$$C_q = \frac{55}{48\sqrt{3}} \frac{\hbar}{m_e c} = 3.83 \cdot 10^{-13} \ \text{m} \ , \tag{2.9}$$

with $2\pi\hbar$ being the Planck's constant, and

$$\mathcal{H} = \frac{1}{\beta_x} \left[ D^2 + \left( \beta_x D' - \frac{\beta_x'}{2} D \right)^2 \right] \ . \tag{2.10}$$

Here $\beta_x$ and $\beta_x'$ are the Courant-Snyder horizontal betatron amplitude function and its derivative, and $D'$ is the derivative of the dispersion function $D$.

Since $\mathcal{H}$ is proportional to $L\theta^2 = \rho\theta^3$, where $\theta$ is the bending angle per half cell of length $L$, the average of the $\mathcal{H}$ function obeys a scaling law:

$$\langle \mathcal{H} \rangle = \mathcal{F} \rho \theta^3 . \tag{2.11}$$

The scaling factor $\mathcal{F}$ depends on the storage-ring lattice arrangement. Possible lattice design of electron storage rings are FODO cells, the double-bend achromat (DBA) or the Chasman-Green lattice, and the triple-bend achromat (TBA) [18]. For FODO-cell lattice, the $\mathcal{F}$ factor is given by

$$\mathcal{F}_{FODO} = \frac{1 - \frac{3}{4}\sin^2\frac{\Phi}{2}}{\sin^3\frac{\Phi}{2}\cos\frac{\Phi}{2}} \ , \tag{2.12}$$

which assumes a minimum of 0.129 when the phase advance per cell is $\Phi = 138°$. The normalized natural rms emittance is given by

$$\epsilon_{\rm nat,n} = \mathcal{F} C_q \frac{\gamma^3 \theta^3}{J_x} \ . \tag{2.13}$$

We can also choose a full coupling between the horizontal and vertical phase spaces; the normalized natural rms emittances in the respective directions are therefore

$$\epsilon_x = \epsilon_z = \frac{1}{2} \epsilon_{\rm nat} \ . \tag{2.14}$$

Synchrotron radiation also leads to a natural rms momentum spread of the electrons, given by

$$\left(\frac{\sigma_E}{E_0}\right)^2 = \frac{C_q\gamma^2}{J_s\left\langle 1/\rho^2\right\rangle}\left\langle\frac{1}{|\rho|^3}\right\rangle \ . \tag{2.15}$$

For an isomagnetic ring, we obtain

$$\left(\frac{\sigma_E}{E_0}\right)^2 = C_q\frac{\gamma^2}{J_s\rho} \ . \tag{2.16}$$

The electron bunch length needs to be adjusted to cover the ion bunch.

## B. CONCEPT OF BEAM TEMPERATURE

The temperature is a thermodynamical quantity in the equilibrium state. But a beam may not ever attain thermodynamic equilibrium. However, a beam is composed of a group of particles where particle motions obey Hamilton's equations[‡]. Beam particles will also occasionally suffer intrabeam Coulomb scattering, beam gas scattering, rf noise, etc. Thus the beam has a thermodynamic-like velocity distribution. We can therefore assign temperatures to the ensemble of beam particles, and relate them to the velocity fields of phase-space coordinates. The transverse and longitudinal temperatures $T_\perp$ and $T_\parallel$ in the beam rest frame are given by [1]

$$kT_\perp = \frac{1}{4}mc^2\beta^2\gamma^2\left(\sigma_{x'}^2+\sigma_{z'}^2\right) \ , \tag{2.17}$$

$$kT_\parallel = \frac{1}{2}mc^2\beta^2\left(\frac{\sigma_p}{p_0}\right)^2 \ , \tag{2.18}$$

where $k$ is the Boltzman's constant, $\sigma_{x'}$ and $\sigma_{z'}$ are the rms divergences of the betatron motions, $\sigma_p/p_0$ is the rms momentum spread of the beam, while $\gamma$ and $\beta$ are the relativistic Lorentz factors. Note that the transverse and the longitudinal temperatures of the electrons in the beam frame are proportional to $\gamma^4$ and $\gamma^2$, respectively, according to Eqs. (2.8) and (2.15). On the other hand, it is interesting to point out that, without consideration of intrabeam scattering, the transverse temperature of the ions increases as $\gamma$, while the longitudinal temperature decreases as $\gamma^{3/2}$ when the rf voltage is kept constant.

[‡]Strictly speaking, electrons obey the Fokker-Planck equation. At equilibrium, however, the effects of quantum excitation and synchrotron damping cancel out, and the electrons follow approximately the Hamiltonian contours [19].

We note that the transverse temperature varies along the circumference of the ring. Since

$$\sigma_{y'}^2 = \frac{1 + \frac{1}{4}\beta_y'^2}{\beta_y}\epsilon_y \ ,$$

where $y$ stands for either $x$ or $z$, the transverse temperature is smaller at the higher-betatron-function locations. This means that beam particles are moving relatively more parallel to each other at these locations. For the sake of avoiding unnecessary complication, we will use in this study the *average* transverse temperature of the beam defined by the *average* beta function $\langle\beta_y\rangle = R/\nu$, where $R$ is the average radius, and $\nu$ is the tune of the machine. An optimized design of the cooling section can further increase the cooling rate.

## C. COOLING RATE ESTIMATION

When two ensembles are mixed together, they will exchange energy through collisions until an equilibrium state of equal temperature is reached. Electron cooling can be viewed as the exchange of kinetic energy between the hot ions and cold electrons through Coulomb scattering. The non-magnetized cooling rate is given by the modified Spitzer formula [1],

$$\alpha_{\text{cool}} = \frac{3\pi Z^2 r_i r_e c n_e \Lambda_c}{\sqrt{2}\gamma^2 \left[2\left(\frac{kT_e}{m_e c^2}\right)^{3/2} + \left(\frac{kT_i}{m_i c^2}\right)^{3/2}\right]} \times \frac{L_c}{C_i}, \tag{2.19}$$

where $m_i$, $Z$, $r_i$, and $T_i$ are the mass, charge, classical radius, and temperature of the ions, and $m_e$, $r_e$, $T_e$, and $n_e$ are the mass, classical radius, temperature, and the density of cooling electrons. The Coulomb logarithmic cutoff term is denoted by $\Lambda_c$, and is chosen to be $\Lambda_c = 10$ in the later cooling-rate estimations. For the electron cooling of the ion beam in a storage ring, the cooling rate is reduced by a factor $L_c/C_i$, where $L_c$ is the length of the cooling section, and $C_i$ is the circumference of the ion ring. In the cooling-rate formula of Eq. (2.19), the transverse cross-sections of electron beam and ion beam are assumed to overlap with each other completely. If they overlap only partially, the cooling rate should be multiplied by an appropriate overlapping factor for cooling reduction. The $\gamma^2$ factor in the denominator comes from the fact that the cooling formula is derived from exchanges of momenta in all directions through

Coulomb scattering in the rest frame of the electron and ion beams. Viewing the process in the laboratory frame, the cooling rate receives one $\gamma$ from time dilation and another one from the electron density as a result of Lorentz contraction. These $\gamma$'s reduce the interest of employing electron cooling at high energies considerably. However, because of the small beam size of the stored electron beams, the electron-beam density $n_e$ can be increased tremendously to provide reasonable cooling rates.

It is also worth pointing out that the transverse temperature in the beam frame is always much higher that the longitudinal temperature. In our later cooling-rate estimation, we assume that the longitudinal plane is decoupled from the transverse planes. This means that the Spitzer cooling time in the longitudinal plane depends only on the longitudinal temperature. The estimation of the basic cooling rates for some storage rings will be discussed in next section.

# III. ELECTRON COOLING FOR ION STORAGE RINGS

## A. TEVATRON AT FERMILAB

The Tevatron is a superconducting proton-antiproton collider at Fermilab. The mean radius is 1 km. The maximum energy is about 1 TeV. The transition gamma is 18.9 and the tune is about 20.6. Here, we assume that two separate and almost identical electron rings are to be constructed, one to cool the proton beam and one to cool the antiproton beam, although one complex $\infty$-shape electron ring may also be possible to cool the two beams at the same time. Parameters of proton/antiproton storage ring and the corresponding cooling electron storage rings are listed in Table I. The second column shows the proton/antiproton beam properties, where we have assumed that the 95% emittances of proton and antiproton beams are 10 $\pi$ mm-mrad (normalized) and 1.5 eV-sec respectively. The harmonic number is 1113 for the Tevatron and 6 for each cooling electron ring. However, the buckets of each electron ring are 3 times as long as those of the Tevatron. The Tevatron runs at an rf voltage of 4 MV.

For the Tevatron, the properties for one cooling electron ring are listed in the third column, where the electron damping time is about 80 ms. It is worth noting

Table I: Properties of the Tevatron, Recycler, and their electron cooling rings.

| | Tevatron | | Recycler | |
|---|---|---|---|---|
| | p or pbar | electrons | p or pbar | electrons |
| $E$ (GeV) | 1000 | 0.544617 | 8.9383 | 0.004868 |
| $p_0$ (GeV/c) | 999.9996 | 0.544617 | 8.8889 | 0.004841 |
| $\gamma$ | 1065.789 | 1065.789 | 9.5263 | 9.5263 |
| $\beta$ | 1.000000 | 1.000000 | 0.994475 | 0.994475 |
| $B\rho$ (Tm) | 3335.639 | 1.816661 | 29.6501 | 0.016148 |
| $B$ (T) | | 0.5 | | 0.025 |
| $\rho$ (m) | | 3.633329 | | 0.6459 |
| $U_0$ (eV) | | 2142.0 | | 0.000077 |
| $\theta$ | | 0.174533 | | 0.785398 |
| $C$ (m) | 6283.185 | 101.615 | 3319.4 | 39.51667 |
| $n_e(\mathrm{m}^{-3})$ | | $2 \times 10^{16}$ | | $1.77 \times 10^{13}$ |
| Beam Radius (mm) | 0.695 | 0.835 | 7.96 | 9.55 |
| $I_{\mathrm{peak}}$ (A) | | 2.10 | | 0.151 |
| $\epsilon_{\mathrm{rms}}$ ($\pi$ mm-mrad) | 1.667 | 1.727 | 5 | 5† |
| $\sigma_p/p_0$ | 0.000110 | 0.000245 | 0.000720 | 0.002† |
| $t_d$ (s) | | 0.0862 | | 8334 |
| $T_\perp$ (eV) | 16167 | 6.56 | 1112 | 1.2† |
| $T_\parallel$ (eV) | 5.63 | 0.0153 | 246 | 1.0† |
| $L_c$ (m) | | 10 | | 10 |
| $\Lambda_c$ | | 10 | | 10 |
| $\Delta\nu_{\mathrm{sc}}$ | | $-0.00051$ | | $-0.0996$ |
| $\lvert Z_\parallel/n\rvert$ (Ohms) | | 2.71 | | 13.4 |
| $\alpha_\perp$ | 0.0000533 $\mathrm{h}^{-1}$ | 5.80 $\mathrm{s}^{-1}$ | 0.0657 $\mathrm{h}^{-1}$ | 0.216 $\mathrm{h}^{-1}$ |
| $\alpha_\parallel$ | 0.805 $\mathrm{h}^{-1}$ | 11.6 $\mathrm{s}^{-1}$ | 0.0326 $\mathrm{h}^{-1}$ | 0.431 $\mathrm{h}^{-1}$ |

†Assumed values at injection.

In the above, $U_0$ is the energy loss per turn, $B$ the magnetic flux density, $\theta$ the dipole magnet bending angle, $C$ the circumference, $n_e$ the electron beam density, $\epsilon_{\mathrm{rms}}$ the rms normalized emittance in $x$ or $z$ direction, $t_d$ the synchrotron radiation damping time, $T_\perp$ and $T_\parallel$ the transverse and longitudinal temperatures, $L_c$ the length of the cooling section, $\Delta\nu_{\mathrm{sc}}$ the Laslett tune spread, $|Z_\parallel/n|$ the longitudinal microwave instability limit assuming $\gamma_t = 6$, and $\alpha_\perp$ and $\alpha_\parallel$ the cooling rates.

that the transverse and the longitudinal cooling rates are dominated by the electron temperatures. Because the electron temperature is still reasonably low, the longitudinal cooling rate is about 1.2 hr while the transverse cooling rate is small due to the large transverse temperatures of both the electron and the proton/antiproton beams. With the combination of a fast longitudinal cooling and the intrabeam scattering, the transverse cooling may be enhanced by a process called sympathetic cooling, where the heat is being transferred from the transverse to the longitudinal degree of freedom. However, since the Tevatron operates above the transition energy, this enhancement may not be significant.

Because of the high Lorentz gamma, the natural emittance of the electron beam will be large according to Eq. (2.13). To minimize it, we choose $\mathcal{F} = 1.4$, which is close to the minimum achievable for FODO-cell lattices. The natural emittance can be further reduced by reducing the bending angle of each dipole. In order for the electron beam to overlap the proton/antiproton beam, the electron rms normalized transverse emittance is chosen to be 1.73 $\pi$ mm-mr, roughly the same as that of the proton/antiproton beam. At the cooling section, the electron beam has a radius of 0.835 mm which is about 20% larger than the proton or antiproton beam. This is achieved by designing the lattice of the electron ring in such a way that the horizontal betatron amplitude function at the cooling section is about 72 m.

The electron bunch length will be adjusted to be slightly longer than the proton/antiproton bunch length. In a bucket, the rms length $\sigma_s$ and the rms momentum spread $\sigma_\delta$ of a bunch are related to the maximum momentum spread $\hat{\delta}$ of the bucket and the rf wavelength $\lambda_{\rm rf}$ (or bucket length) by

$$\frac{\hat{\delta}}{\sigma_\delta} = Y(\phi_s)\frac{\lambda_{\rm rf}}{\pi\sigma_s} , \tag{3.1}$$

where $Y(\phi_s)$ is a function of the synchronous phase $\phi_s$ and is close to unity when $\phi_s$ is small. Note that this formula is independent of the rf voltage and the slippage factor. Therefore, for the same rf wavelength, it applies to both the proton/antiproton and electron bunches. This implies that the matching of the bunch lengths of the two bunches is the same as the matching of their ratios of momentum spreads to bucket heights. For the Tevatron, the bucket to rms bunch momentum spread is $k = 8.25$ when the rf voltage is at 4 MV and the bunch area is 1.5 eV-s. If the electron bunch length is 20% longer than the proton/antiproton bunch length, the bucket height to

rms bunch height will become $8.25/1.2 = 6.88$, which may be a bit too small for the electron bunch. This is because there is a finite quantum lifetime for electron bunches as a result of quantum excitation. For this reason, we have chosen the electron bucket length to be three times the proton/antiproton bucket length; or $n = 3$ in Eq. (1.1). In order that this design is possible, we must ensure that every Tevatron bunch will meet with a cooling electron bunch in every revolution. The first requirement is that the Tevatron rf harmonics $h_i$ must be a multiple of $n = 3$. At the same time, we also require the Tevatron bunches to be placed only in the 0th, 3rd, 6th, 9th, $\cdots$ consecutive buckets. Since $h_i = 1113$ for the Tevatron, the first requirement is satisfied. The second requirement is also fulfilled in the $36 \times 36$ colliding scheme, where the Tevatron bunches occupy only every 21st bucket. In the $99 \times 99$ scheme, however, the bunches occupy every 7th bucket which is not a factor of $n = 3$, implying that two thirds of the Tevatron bunches will never see an electron bunch or will never be cooled. To remedy this, the Tevatron bunch spacing should be changed to every 6th bucket instead in this colliding mode. If not, the bucket length of the electron ring must be set back to equal one Tevatron bunch length, or 7 Tevatron bunch lengths. For the latter arrangement, the rf harmonics and the circumference of the electron ring also need to be modified.

Now with $n = 3$, the bucket height to rms bunch height for the electron bunches increases to $k = 20.6$. The shift of the synchronous angle $\phi_s$ to compensate for the radiation loss $U_0$ per turn is given by

$$\phi_s = \tan^{-1}\left(\frac{2U_0}{\pi\beta^2\eta h_e k^2 \sigma_\delta^2 E_e}\right) = 0.533 \text{ rad} , \tag{3.2}$$

where $E_e$ is the energy of the electrons and the transition gamma of $\gamma_t = 6$ has been assumed for the electron ring giving a slip factor of $\eta = 0.0278$. The required rf for the electron ring is then

$$V_{\rm rf} = \frac{U_0}{\sin\phi_s} = 4.22 \text{ kV} . \tag{3.3}$$

The electron bunch, having such a long bunch length, can be subject to longitudinal microwave instability, with a threshold given by [20]

$$\left|\frac{Z_\parallel}{n}\right| = \frac{2\pi\beta^2 E\sigma_\delta^2\eta F}{eI_{\rm peak}}, \tag{3.4}$$

where $I_{\rm peak}$ is the peak current, and the form factor $F \approx 1$ for Gaussian beam. Using parameters listed in Table I, we find $|Z_\parallel/n| \approx 2.7$ Ohm.

## B. RECYCLER AT FERMILAB

For the Recycler, the goal of stochastic cooling or electron cooling is to recycle unused antiprotons from the Tevatron and accumulate and cool newly produced pre-cooled antiprotons from the Accumulator [9]. Parameters of the ion and the cooling electron storage rings are listed in the 4th and 5th columns of Table I. Here, we have assumed that the 95% normalized emittances of the recycled antiproton beam are 30 $\pi$ mm-mrad and 150 eV-sec, where the corresponding rms transverse and longitudinal temperatures are 1112 eV and 245 eV, respectively. The goal of the cooling is to attain the 95% emittances of 10 $\pi$ mm-mrad (normalized) and 50 eV-s, respectively.

At 8.9 GeV antiproton energy, the electron cooling storage ring is 4.87 MeV. The corresponding damping time for the cooling electrons is about 2 hrs. We therefore assume that the freshly injected accumulated cooling electrons in the cooling storage rings have a normalized rms emittance of 5 $\pi$ mm-mrad and an rms momentum spread of $\pm 0.2\%$. This corresponds to transverse and longitudinal temperatures of 1.2 eV and 1.0 eV respectively. These cooling electrons will be replenished at a fixed interval to be determined by the cooling rate and the intensity of electron beam attainable in the ring. With this choice of electron beam properties, the cooling rates are determined mainly by the electrons during the injection process.

The beam intensity of this low-energy electron storage ring can be limited by the incoherent space-charge tune shift, which is given by [21]

$$\Delta\nu_{\rm sc} = -\frac{N_e r_e C_e}{4\pi\beta^2\gamma^3\epsilon_e} \ , \tag{3.5}$$

where $N_e$ is the number of electrons per unit length, $C_e$ is the circumference of the electron storage ring, $\epsilon_e$ is the unnormalized rms emittance of electron beam. For an order of magnitude estimation with a $-0.1$ space-charge tune shift, the maximum electron current allowed is about $N_e = 3 \times 10^9$ e/m. If the electron beam radius at the cooling section is 10 mm, the resulting electron density will be limited to about $n_e = 1 \times 10^{13}$ m$^{-3}$. The resulting longitudinal antiproton cooling time is too long to be useful. A possible alternative scenario is to cool antiprotons with electrons freshly produced from a source and accelerated to the proper energy by means of a pelletron. In this single-pass system, the space charge tune shift plays no role and the electron charge density can therefore be increased to attain a higher cooling rate.

## C. RHIC AT BNL

RHIC is a heavy ion collider with 200 GeV/u center-of-mass energy for Au+Au. It can also be used for proton collision at the center-of-mass energy of 500 GeV. At 100 GeV/u, the ion beams suffer tremendous emittance growths in both the longitudinal and transverse directions. This is because the intrabeam-scattering growth rates are proportional to $Z^4/A^2$, where $Z$ is the ion charge and $A$ its nucleon number. This amounts to, for example, a factor of $79^4/197^2 = 1004$ for the gold ion beam, and the growth times [22] are only 9 and 27 minutes, respectively, in the longitudinal and transverse directions. We therefore need to maximize the respective electron cooling rates in order to ensure the stability of the ion beams.

Furthermore, at this lower ion energy, the space-charge force for the intense cooling electron beam will also be important. Here, we try to to maintain a tune shift of about $-0.1$ by minimizing the peak current of the electrons through the reduction of the beam size. In this way, a peak electron density as high as $n_e = 2 \times 10^{16}$ m$^{-3}$ can still be applied, and high cooling rates can therefore be possible.

Parameters of RHIC and its corresponding cooling electron storage ring are listed in Table II. The circumference of the electron ring is chosen to be 50.2 m, having an rf harmonic of $h_e = 11$, so that each electron rf bucket matches three bucket lengths ($n = 3$) of the ion ring. This is possible because the ion ring, running at an rf voltage of 4 MV, has a harmonic number of 2520 which is a multiple of $n = 3$. At the same time, the bunch spacing of the ion bunches should also be a multiple of 3 bucket lengths, so that every ion bunch will meet with a cooling electron bunch in every revolution. This choice of $n$ is necessary because each ion bunch is very large and fills up most of the bucket. For example, the bucket height to rms bunch height is only $k = 3.44$ in the 250 GeV operation and $k = 6.28$ in the 100 GeV Au operation. Enlarging the electron bucket length by three times enhances the electron bucket height to rms bunch height to 8.61 and 9.80 for the two operations. According to Eqs. (3.2) and (3.3), the synchronous phases are, respectively, 0.0185 and 0.000158 rad for the two operations, while the rf's are, respectively, 0.906 and 2.705 kV. If necessary, the ratios bucket to rms bunch heights can be further increased by raising the electron bucket length to five times the ion bucket length. However, the rf harmonic needs also to be adjusted to, for example $h_e = 7$, so that the circumference of the electron ring, which

Table II: Properties of the RHIC and its electron cooling ring at 2 energies.

| | protons | electrons | protons (heavy ions) | electrons |
|---|---|---|---|---|
| $E$ (GeV) | 250 | 0.136154 | 100 | 0.054462 |
| $p_0$ (GeV/c) | 249.9982 | 0.136154 | 99.9956 | 0.054460 |
| $\gamma$ | 266.4472 | 266.4472 | 106.5789 | 106.5789 |
| $\beta$ | 0.999993 | 0.999995 | 0.999956 | 0.999956 |
| $B\rho$ (Tm) | | 0.454162 | | 0.181658 |
| $B$ (T) | | 0.25 | | 0.099996 |
| $\rho$ (m) | | 1.816634 | | 1.816649 |
| $U_0$ (eV) | | 16.73 | | 0.428423 |
| $\theta$ | | 0.418879 | | 0.418879 |
| $C$ (m) | 3833.85 | 50.2051 | 3833.85 | 50.2051 |
| $n_e$ ($m^{-3}$) | | $2 \times 10^{16}$ | | $2 \times 10^{16}$ |
| Beam radius (mm) | 0.886 | 1.234 | 1.40 | 1.75 |
| $I_{\rm peak}$ (A) | | 4.60 | | 9.19 |
| $\epsilon_{\rm rms}$ ($\pi$ mm-mrad) | 1.667 | 2.13 | 1.667 | 1.705 |
| $\sigma_p/p_0$ | 0.000452 | 0.000432$^\dagger$ | 0.000493 | 0.000692$^\dagger$ |
| $t_d$ (s) | | 1.36 | | 21.3 |
| $T_\perp$ (eV) | 9970 | 4.57 | 3988 | 1.46 |
| $T_\parallel$ (eV) | 96.0 | 0.0478$^\dagger$ | 114 | 0.122$^\dagger$ |
| $L_c$ (m) | | 10 | | 10 |
| $\Lambda_c$ | | 10 | | 10 |
| $\Delta\nu_{\rm sc}$ | | $-0.00712$ | | $-0.111$ |
| $\lvert Z_\parallel/n\rvert$ (Ohms) | | 0.97 | | 1.11 |
| $\alpha_\perp$ | 0.00259 $h^{-1}$ | 0.367 $s^{-1}$ | 0.07744 $h^{-1}$ | 0.0235 $s^{-1}$ |
| $\alpha_\parallel$ | 2.54 $h^{-1}$ | 0.734 $s^{-1}$ | 5.16 $h^{-1}$ | 0.0470 $s^{-1}$ |

$^\dagger$The momentum spreads have been increased 5 folds from the natural spreads to avoid longitudinal microwave instability.

In the above, $U_0$ is the energy loss per turn, $B$ the magnetic flux density, $\theta$ the dipole magnet bending angle, $C$ the circumference, $n_e$ the electron beam density, $\epsilon_{\rm rms}$ the rms normalized emittance in $x$ or $z$ direction, $t_d$ the synchrotron radiation damping time, $T_\perp$ and $T_\parallel$ the transverse and longitudinal temperatures, $L_c$ the length of the cooling section, $\Delta\nu_{\rm sc}$ the Laslett tune spread, $|Z_\parallel/n|$ longitudinal microwave instability limit assuming $\gamma_t = 6$ and 4 for the two operations, and $\alpha_\perp$ and $\alpha_\parallel$ the cooling rates.

becomes $C_e = 53.248$ m, remains an integral number of the ion bucket length. Also, the bunch spacing of the ion bunches must be chosen to be a multiple of 5 bucket lengths. The cooling times will be slightly modified accordingly.

Since intrabeam scattering will be most severe for the 100 GeV/u operation, we would like to optimize the electron cooling ring for this operation. We would like to obtain a large transverse electron beam size and a small average betatron function (or a large emittance), so that we can accommodate a high electron density with the Laslett tune shift kept at $\sim -0.1$. The horizontal betatron function at the cooling section is set at 31.7 m. The natural emittance will be small due to a small Lorentz gamma. To obtain a large emittance for the electron bunches, we choose $\mathcal{F} = 100$ for the lattice and limit the number of dipoles to 15. Such a larger $\mathcal{F}$ is feasible from a weakly focused storage ring. Then, in the cooling section, the electron beam radii are 4.35 and 1.75 mm, respectively, for the 250 GeV and 100 GeV operations, whereas the ion beam radii are, respectively, 0.886 and 1.40 mm. The electron beam radius and emittance appear to be large for the 250 GeV operation. Also, the peak current is 57.5 Amp which is too high. This is because an electron ring optimized for the 100 GeV/u operation is used here. However, it is possible to modify the lattice of the electron ring during the 250 GeV operation by increasing the currents in the quadrupoles, making the ring more focusing. For example, if we can alter the ring to $\mathcal{F} = 8$, the rms normalized emittance of the electron bunch will decrease from $26.64 \times 10^{-6}\pi$ m to $2.13 \times 10^{-6}\pi$ m, and the electron beam radius will become 1.23 mm. Also such a modification can also bring down the peak current of the electron bunch to 4.50 Amp with the decrease in the transverse bunch size. This will certainly be beneficial to the stability issues of the electron bunches.

We find that the electrons at both energies are too cold and will suffer from longitudinal microwave instability. As a result, we propose the installation of an undulator so that the momentum spreads will be blown up by a factor of 5 from the natural values. The stability limits against longitudinal microwave instability become 1.55 and 1.11 Ohms for the two operation energies, where transition gammas of $\gamma_t \approx 6$ and 4 have been assumed. At both operation energies, electrons dominate in the longitudinal Spitzer cooling rates, but both the ions and electrons contribute almost equally to the transverse cooling rates.

We find from Table II that the Spitzer cooling times at the 250 GeV operation

energy are about 24 min longitudinally and rather long transversely. Since only protons are stored at this energy, the transverse intrabeam scattering growth time is relatively small and the cooling will be quite adequate. At 100 GeV/u, the ion damping times are about 12 min longitudinally and 12.9 hr transversely. However, these are per nucleon numbers. At a fixed rf voltage and a fixed longitudinal emittance per nucleon, the momentum spread should be multiplied by a factor of $(Z/A)^{1/4}$ due to the change in synchrotron frequency. The final cooling rates should be enhanced again by a factor of $Z^2/A$, which equals 31.7 for the gold ions. The longitudinal and transverse cooling rates then become 0.34 and 24 min, respectively, which should be adequate to counteract the rapid growths due to intrabeam scattering in both directions. Transverse cooling is possible here because of the enhancement factor of $Z^2/A$, the lower $\gamma$, and the lower transverse temperature of the electrons.

From the above estimation of the ion beam cooling rates, cooling electron storage ring is economical and effective in providing beam cooling for RHIC.

# IV. DYNAMICS OF ELECTRON COOLING WITH ELECTRON STORAGE RINGS

The cooling of ion beams using electrons can be visualized as the temperature equilibration between two plasmas. Let $T_e$, $T_p$, $N_e$, and $N_p$ be respectively the temperatures and number of particles of two plasmas. If we mix these two plasmas together, the temperature of the plasmas will be equilibrated to reach a temperature of $(N_eT_e+N_pT_p)/(N_e+N_p)$. The cooling time is equal to inverse of the Spitzer cooling rate of Eq. (2.19), if only Coulomb scattering is considered.

However, electrons in the storage ring emit synchrotron radiation. The synchrotron radiation together with the energy compensation from the rf cavities provide damping to the electron beams. Since synchrotron radiation is a quantum process, the quantum fluctuation and damping produce an equilibrium temperature.

With the inclusion of radiation damping, the proton beam will still reach the same temperature as that of electrons when they are mixed together. However, protons and ions suffer from strong intrabeam scattering. Without cooling, the proton beam will grow indefinitely. The growth rate depends on the phase space density of the

proton beams. Observation at the Tevatron and theory prediction show that the growth rate of the longitudinal momentum spread is inversely proportional to the third power of the momentum spread [23]. Here, for the sake of illustration, we follow a simplified model where the longitudinal momentum spread grows according to the inverse square of the momentum spread instead. In term of temperature, the growth rate can therefore be approximated by a constant.

Combining all these effects, we can write down the equations of state as follows:

$$\frac{dT_e}{dt} = \frac{1}{\tau_c}\frac{N_p}{N_e+N_p}(T_p - T_e) - \frac{2}{\tau_d}(T_e - T_0) \ , \tag{4.1}$$

$$\frac{dT_p}{dt} = -\frac{1}{\tau_c}\frac{N_e}{N_e+N_p}(T_p - T_e) + G \ , \tag{4.2}$$

where $\tau_c$ is the Spitzer cooling time, $\tau_d$ is the synchrotron radiation cooling time, $T_0$ is the equilibrium temperature of electrons, and $G$ is the intrabeam scattering heating rate. For the Tevatron, $G$ is roughly 4 eV per 12 hours. The system of equations can be solved easily to obtain an equilibrium solution given by

$$T_{e,\mathrm{eqb}} = T_0 + \frac{N_p}{2N_e}G\tau_d \ . \tag{4.3}$$

$$T_{p,\mathrm{eqb}} = T_0 + \frac{N_p}{2N_e}G\tau_d + \frac{N_p+N_e}{N_e}G\tau_c \ . \tag{4.4}$$

Note that the final temperatures of electron and ion beams are now different, and they can be controlled by adjusting the number of electrons relative to proton beams. The instantaneous solution can also be obtained easily. It can be written as

$$\begin{pmatrix} T_e \\ T_p \end{pmatrix} = \begin{pmatrix} T_{e,\mathrm{eqb}} \\ T_{p,\mathrm{eqb}} \end{pmatrix} + \begin{pmatrix} a_1 \\ b_1 \end{pmatrix} e^{\lambda_1 t} + \begin{pmatrix} a_2 \\ b_2 \end{pmatrix} e^{\lambda_2 t} \ , \tag{4.5}$$

where $a_1$ and $a_2$ are determined by the initial electron and proton temperatures, while $b_1$ and $b_2$ are functions of $a_1$ and $a_2$. The two eigenvalues are given by

$$\lambda_{1,2} = -\frac{1}{2}\left(\frac{1}{\tau_c}+\frac{2}{\tau_d}\right) \mp \sqrt{\frac{1}{4}\left(\frac{1}{\tau_c}+\frac{2}{\tau_d}\right)^2 - \frac{2}{\tau_c\tau_d}\frac{N_e}{N_p+N_e}} \ , \tag{4.6}$$

and are both negative. Radiation damping is in general very much faster than the Spitzer cooling rate; the two eigenvalues then become

$$\lambda_1 \approx -\frac{2}{\tau_d} \quad \text{and} \quad \lambda_2 \approx -\frac{1}{\tau_c}\frac{N_e}{N_p+N_e} \ . \tag{4.7}$$

The terms corresponding to the eigenvalue $\lambda_1$ decay rapidly in a time period equal roughly to one half the radiation damping time. For the protons, the coefficient $b_1$ is very much less than $b_2$. The real cooling therefore comes from the term associated with the second eigenvalue $\lambda_2$, which, as was stated in Eq. (4.7), provides a cooling rate always less than the Spitzer cooling rate. It is interesting to point out that this reduction comes from the presence of radiation damping but not from intrabeam scattering. However, this cooling rate can be enhanced by increasing the proportion of electrons in the two plasmas.

# V. CONCLUSION

In conclusion, we have analyzed the feasibility of using an electron storage ring as a cooling device for hadron colliders and storage rings. The longitudinal cooling times estimated are based on the Spitzer equilibration time, with the assumption that the longitudinal cooling times depend only on the longitudinal temperatures. We find that, with the exception of the Recycler, the longitudinal cooling rates are relatively moderate due to the smaller longitudinal temperatures of circulating beams. With careful choice of electron beam parameters and the ratio of electron beam intensity to that of proton beam intensities, high energy colliders can attain cooling from electron storage rings. However, the transverse cooling rates per nucleon for high energy colliders, such as the Tevatron and RHIC, are relatively slow. This is not important for the Tevatron because the transverse emittance growth time is of the order of a store, and hopefully the transverse cooling rates will be enhanced from the sympathetic cooling mechanisms, such as intrabeam scattering, synchro-betatron coupling, etc. RHIC, on other hand, has transverse growth rate of the order of only half an hour due to the high charge of the gold ions. However, the the cooling rates are also enhanced by the factor $Z^2/A = 32$ making transverse cooling possible. It appears that the high energy ion colliders can benefit most from electron cooling storage rings.

Electron electron rings can be designed in race-track FODO lattices. In each case, the electron bucket spacing should be chosen as an integral multiple of the bucket spacing of the ion storage ring. In our analysis, we have used simple FODO-type accelerators in order to increase the electron beam emittances. For each ion

storage ring or collider, the actual electron beam emittance and the beam size at the cooling section have to be optimized in a detailed lattice design. Furthermore, evolution of ion and electron beam distributions, and other beam dynamics issues of the electron cooling storage rings should be carefully studied for better understanding of the cooling process.

## ACKNOWLEDGMENTS

We wish to thank A. Gerasimov and J. MacLachlan for their helpful comments. This work was supported by grants from NSF PHY-9221402 and DOE DE-FG02-92ER40747.

# References

[1] H. Poth, Phys. Reports **196**, 135 (1990).

[2] R.E. Pollock, Ann. Rev. Nucl. Sci. **41**, 357 (1991).

[3] G.I. Budker *et al.*, Particle Accelerators, **7**, 197 (1976);

[4] D.D. Caussyn *et al.*, Phys. Rev. Lett. **73**, 2857 (1994).

[5] D.D. Caussyn *et al.*, Phys. Rev. **E51**, 4947 (1995).

[6] S.Y. Lee *et al.*, Phys. Rev. **E52**, to appear (1995).

[7] S.Y. Lee, *et al.*, Phys. Rev. Lett. **67**, 3768 (1991); D.D. Caussyn *et al.*, Phys. Rev. **A46**, 7942 (1992); J.Y. Liu *et al.*, Phys. Rev. **E49**, 2347 (1994); M. Ellison *et al.*, Phys. Rev. **E50**, 4051 (1994).

[8] M. Ellison, *et al.*, Phys. Rev. Lett. **70**, 591 (1993); H. Huang *et al.*, Phys. Rev. **E48**, 4678 (1993); D. Li, *et al.*, Phys. Rev. **E48**, R1638 (1993); M. Syphers *et al.*, Phys. Rev. Lett. **71**, 719 (1993); Y. Wang *et al.*, Phys. Rev. **E49**, 1610 (1994); J.Y. Liu *et al.*, Phys. Rev **E50**, R3349 (1994); J.Y. Liu *et al.*, Particle Accelerators, **49**, 221 (1995); D. Li, *et al.*, Nucl. Inst. Meth. **A364**, 205 (1995).

[9] G. Jackson, Fermilab Internal Report TM-1991 (1996).

[10] G. Jackson, *Proc. 1993 Particle Accelerator Conf*, Washington, D.C., May 17-20, 1993, p. 3533.

[11] F. Mills, private communication.

[12] C. Rubbia, *Proc. of the Workshop on Producing High Luminosity High Energy Proton-Antiproton Collisions*, Berkeley, March 27-31, 1978, (LBL-7574, 1978), p. 98.

[13] A.G. Ruggiero, *ibid.*, p. 166 (1978).

[14] T. Ellison, Nucl. Inst. Meth. **A364**, 27 (1995).

[15] A. Piwinski, *Proc. 9th Int. Conf. on High Energy Accelerators*, Stanford, 1974, p. 405; J.D. Bjorken and S.K. Mtingwa, Particle Accelerator **13**, 115 (1983); J. Wei *Proc. 1993 Particle Accelerator Conf*, Washington, D.C., May 17-20, 1993, p. 3651.

[16] D. Finley, Fermilab Internal Report TM-1648 (1989).

[17] C. Bernardini *et al.*, Phys. Rev. Lett. **10**, 407 (1963).

[18] S.Y. Lee, Phys. Rev. **E54**, 1940 (1996).

[19] M. Bai, *et al.*, Phys. Rev. **E55**, 3493 (1997).

[20] S. Krinsky and J.M. Wang, Part. Accel. **17**, 109 (1985).

[21] See for example, D.A. Edwards and M.J. Syphers, *An Introduction to the Physics of High Energy Accelerators*, Wiley, New York, 1993, p. 176.

[22] J. Wei, private communication.

[23] C. Bhat, P. Colestock, and L. Spentzouris, work in progress.